Materials International
Open Access Journal (ISSN: 2668-5728)

Article
Volume 6, Issue 3, 2024, 25
https://doi.org/10.33263/Materials63.025

Thermodynamic and Kinetic Study of Corrosion Inhibition of Mild Steel by Plant Extract in Acidic Medium

Suchitra Chaudhary [1,*], Rakesh K. Tak [1], Kavita Kumari [1], Nikita Sharma [2]

[1] Department of Chemistry, SPCGCA, MDS University, Ajmer (Rajasthan), India
[2] Department of Chemistry, SPNKS Govt PG College, Dausa, University of Rajasthan, Jaipur (Rajasthan), India
* Correspondence: e suchitra_gca@yahoo.com (S.C.);

Scopus Author ID 57194602277
Received: 20.05.2022; Accepted: 27.05.2023; Published: 10.09.2024

Abstract: The effect of the inhibitor on the corrosion behavior of mild steel in sulphuric acid is directly dependent on the concentration of Tribulus *terrestris* fruit extract (TTFE) dissolved in the corrosive solution. The values for corrosion rate obtained in blank solution are much higher than those of inhibited solution for all the immersion time, indicating the existence of a protective film on the corroding surface. Corrosion rate and inhibition efficiency plots of Mild Steel with and without the addition of different concentrations of TTFE in 1.5N H_2SO_4 at 303-333K show that corrosion rate increases with increasing temperature both in uninhibited and in inhibited solutions while the inhibition efficiencies are found to decrease with increasing concentration of the solution. The thermodynamic parameters activation energy, enthalpy, and entropy were calculated from the mass loss measurements, suggesting that the adsorption is spontaneous, the corrosion process is exothermic and obeyed the Langmuir adsorption isotherm. The kinetic parameters were evaluated, and a pseudo-first-order kinetics relationship with respect to mild steel was obtained. The EIS analysis indicates that the corrosion impedance increases with the extract of *Tribulus terrestris* by forming a protective layer on the metal. The plant extract is a mixed-type inhibitor characterized by Taffel analysis. The SEM image of the untreated metal surface shows a smooth metal surface, which indicates the absence of any corrosion product on the metal surface.

Keywords: corrosion, inhibition efficiency; mass loss measurements; Langmuir adsorption isotherm; electrochemical measurements; SEM.

1. Introduction

Mild steel is a very common ferrous alloy, one of the most economical types of steel, having iron with a carbon content between 0.05% - 0.25% by weight and density of almost 7.85 g/cm^{3,} depending on grade. It is the best-preferred construction material in household and industrial materials, for example, in boilerplates, bridge work structures, reactors, automobiles, steam engine parts, etc., all across the world due to its availability, excellent mechanical properties, ease of fabrication, and low purchasing cost [1]. It is also used in most the chemical industries for fabrication material in tanks, reaction vessels, pipelines, capacitors, etc.. Still, due to a lack of alloying elements (like chromium, nickel, and molybdenum, which are found in stainless steel), mild steel is subjected to oxidation (rust) of iron easily.

As it has weak corrosion resistance, the destructive nature of the environment causes the attack of this metal surface by corrosion, which causes metal dissolution, which is considered a prime factor for concern [2]. Highly aggressive acid solutions such as hydrochloric and sulphuric acids have been used for pickling baths, industrial acid cleaning, dealing operations, descaling processes, and oil well acidizing, which is also a big cause of corrosion [3].

The use of corrosion inhibitors is one of the most practical and cost-effective methods to protect materials from corrosion in the industry and extends the lifetime of metallic materials. Unfortunately, many of the inhibitors (organic and synthetic compounds) reported earlier are expensive and hazardous to the environment [4-6]. In recent years, researchers have been more attentive towards using green compounds that are non-toxic, biodegradble, economical, and compatible with current industrial technologies and the environment [7-14].

Tribulus terrestris, a natural herb, is used in the present study to investigate its anticorrosion behavior for mild steel in an acidic medium (H_2SO_4). It is a member of the Zygophyllaceae family and comprises 25 genera and about 250 species worldwide [15,16]. This plant, also known as Gokshura, Chhota Gokshura, or Puncture Vine, is used in different medical applications [17,18] as well as Ayurvedic medicinal herbs [19]. The present work aims to study the alcoholic extract of *Tribulus terrestris* fruit (TTFE) as a safe, economical, non-toxic, and environmentally friendly inhibitor for mild steel corrosion in an acidic solution.

1.1. Phytochemical constituents in Tribulus terrestris fruit extract (TTFE).

The alcoholic fruit extract of *Tribulus terrestris* plant has been used in different concentrations as an inhibitor. Many researchers have already done a previous phytochemical study of Tribulus terrestris. Screening of phytochemical constituents of TTFE was carried out by Vasait Rajendrabhai in 2017 to identify its active constituents. He showed the presence of amino acids, proteins, carbohydrates, glycosides, tannins, terpenoids, phenols, and saponins [20].

Table 1. Phytochemical Analysis of TTFE [20].

Phytochemicals	**Fruit Extracts**	
	Aqueous	Methanol
Carbohydrates	+	+
Amino acids and peptides	+	+
Glycosides	-	+
Tannins	+	+
Terpenoids	-	+
Phenols	-	+
Saponins	+	+

Table 2. GC – MS analysis of *Tribulus terrestris* [21].

S. No.	***RT***	***Name of the compound***	***Molecular Formula***	***Peak Area%***
1	14.52	3,7,11,15-tetramethyl-2-hexadecen-1-o1	$C_{20}H_{40}O$	1.04
2	16.27	n-Hexadecadienoic acid	$C_{16}H_{32}O_2$	8.83
3	16.58	Hexadecadienoic acid, ethyl ester	$C_{18}H_{36}O_2$	0.74
4	18.55	phytol	$C_{20}H_{40}O$	0.99
5	18.86	9,12-Octadecadienoic acid (z,z)-	$C_{18}H_{32}O_2$	1.86
6	18.95	9,12,15-Octadecatrienoic acid, (z,z,z)-	$C_{18}H_{36}O_2$	8.58
7	19.26	Octadecanoic acid	$C_{18}H_{34}O_2$	2.95
8	24.82	1,2-Benzenedicarboxylic acid, disooctyl ester	$C_{24}H_{38}O_4$	9.27
9	31.46	α-Amyrin	$C_{30}H_{50}O$	65.73

Table 1 shows the presence of phytochemicals in the TTFE. The Tribulus terrestris whole plant Methanolic extract studies by GC-MS analysis clearly showed the presence of nine compounds (Table 2) [21].

The presence of all the above phytochemicals has been reported to promote the corrosion inhibition of mild steel in an aggressive acidic solution. [22,23]. Molecules with nitrogen and acetylenic alcohols are claimed to form a film on the metal surface and can retard the metal dissolution process (an anodic reaction) as well as hydrogen evolution (a cathodic reaction) [24]. Previously, the *Tribulus terrestris* plant has been reported to inhibit the corrosion of mild steel in HCl Solution [11,25], H_2SO_4 solutions [10], phosphoric acid solution [26], and aluminum in Hydrochloric acid [27]. The current study, therefore, seeks to investigate the inhibitive and adsorptive characteristics of the methanol extract of TTFE for mild steel corrosion in H_2SO_4.

2. Materials and Methods

2.1. Specimen and solution preparation.

The test specimens were made up of mild steel [MS] alloy with elemental composition, as shown in Table 3.

Table 3. Composition of various elements present in mild steel coupons.

Element	Fe	Cr	S	P	Mn	C
Composition (%)	99.7008	0.0194	0.0128	0.0160	0.1620	0.0890

The test specimens of dimension 1.5 x 2.5 x 0.072 cm^3 were first mechanically polished with the help of emery papers of different grades, then degreased in absolute ethanol, dried in acetone, and weighed. The weights of the specimens before and after corrosion were determined using a digital analytical balance.

The solution of 1.5N H_2SO_4 was made from AR-grade qualigens H_2SO_4 with double-distilled water. The inhibitor was prepared by rinsing the fruit part of the plant in distilled water and drying it in the shade. The dried fruit then powdered and was refluxed with 80% methanol in the Soxhlet apparatus. The extract concentration ranges of fruit used were: 0.12%, 0.24%, 0.36%, 0.48%, and 0.60%. All experiments were executed at 30 ±1 ^{0}C (except experiments for the effect of temperature). The temperature was controlled by a Bacteriological incubator.

2.2. Methods.

The inhibition efficiency of the inhibitor for MS in 1.5N H2SO4 was followed by chemical methods.

2.2.1. Mass loss measurements.

The mass loss measurements were conducted for different time intervals (6, 12, 24, 48, and 72 hrs.) at various temperature ranges from (303 – 333 K) in 1.5N H_2SO_4. The weighted and polished specimens were immersed in 50 mL of solution with and without inhibitor. After the specified time, the specimens were removed from the test solution, thoroughly washed with distilled water, dried out, weighed, and loss in mass was measured for the workout of the impact of different parameters, such as inhibitor concentration, time, and temperature. The percentage of inhibition efficiency (IE%), degree of surface coverage (θ), and corrosion rate for the predefined concentration range of inhibitor were calculated [28] by eq. (1) and (2), respectively.

$$IE\% = \left(\frac{\Delta M_0 - \Delta M}{\Delta M_0}\right) 100 \qquad \ldots(1)$$

$$\theta = \frac{\Delta M_0 - \Delta M}{\Delta M_0} \qquad \ldots(2)$$

Where, ΔM and ΔM_0 are mass loss of metal in the presence and in the absence of inhibitor in acid solution, respectively.

The Corrosion Rate (CR) can be computed [29] by eq. (3).

$$CR = \frac{8.76x10^4 x\Delta M}{A\ x\ T\ x\ D} \qquad \ldots(3)$$

Where CR is in millimeters per year (mmpy), ΔM is in grams, A (area of the specimen) is in cm^2, T (time) is in hours, and D (density of the specimen) is expressed in gcm^{-3}.

2.2.2. Electrochemical measurements.

Gamry Potentiostat/Galvanostat (Model Reference 600) with EIS software is used for electrochemical studies. The cell body consists of three electrodes a working electrode (metal specimen with an area of $1 \times 1cm^2$), an auxiliary electrode (graphite electrode), and a reference (saturated calomel) electrode. The electrochemical studies, including potentiodynamic polarization and electrochemical impedance spectroscopy (EIS) were carried out to evaluate the IE of TTFE in 1.5N H_2SO_4.

The inhibition efficiency in the potentiodynamic polarization method (IE %) obtained by the Tafel extrapolation method is calculated using eq. (4) [27]

$$IE\% = \left(\frac{I^0_{corr} - I_{corr}}{I^0_{corr}}\right) 100 \qquad \ldots(4)$$

Where the corrosion current I^0_{corr} and I_{corr} are in the absence and the presence of inhibitor, respectively, which were carried out by scanning the potential ranging from -100 to 100 mV vs. reference electrode at a scan rate of 1mV per second.

The Randle equivalent circuit [27] program was used for impedance data analysis. The inhibition efficiency is calculated from the charge transfer resistance R_{ct} value using eq. (5) [30]

$$IE\% = \left(\frac{R_{ct} - R^0_{ct}}{R_{ct}}\right) 100 \qquad \ldots(5)$$

Where R^0_{ct} and R_{ct} are the charge transfer resistance in the absence and in the presence of inhibitor, respectively which were carried out at open circuit potential under unstirred conditions with a stabilization period of 30 min for the frequency range from 100 kHz to 0.01 Hz.

2.3. Surface analysis.

The surface morphologies for the MS metal in 1.5N H_2SO_4 solution in the presence and absence of the inhibitors (TTFE) for various immersion times were obtained by scanning electron microscopy (SEM) under the condition of 10 kV acceleration voltage. This was done at MNIT Jaipur, India, using the Nova Nano SEM 450 instrument.

3. Results and Discussion

3.1. Mass loss measurement.

The corrosion rate, surface coverage, and inhibition efficiency can be calculated using different gravimetric parameters obtained by the Mass Loss method at 303±1K.

3.1.1. Effect of TTFE concentration.

The corrosion behavior of mild steel in 1.5N sulphuric acid in the presence and in the absence of TTFE is summarized in Table 4. According to Table 4, the corrosion inhibition efficiency directly depends on the concentration of TTFE dissolved in the corrosive solution. Increasing the concentration of TTFE from 0.12% to 0.60% enhanced the corrosion inhibition efficiency from 73.19% to 89.08% at 303K, and it is also observed that the corrosion rate of MS in H_2SO_4 decreased from 52.38 mmpy in the absence of the inhibitor to 5.72 mmpy in the presence of 0.60% TTFE for 12 hrs immersion period. The results revealed that the strong adsorption of extract molecules on metal surfaces retards the corrosion process [31].

Corrosion reactions are assumed to be nullified from the metal surface covered by adsorbed inhibitory species, while corrosion reactions normally occur in the inhibitor-free area. Therefore, the effectiveness of the inhibition is directly proportional to the fraction of the covered surface of metal [32].

3.1.2. Effect of immersion time.

The data obtained for inhibition efficiency and corrosion rate of MS coupons in sulphuric acid in different periods explain the efficiency of the inhibitory action of TTFE during immersion time.

The corrosion rate values obtained in the blank solution are much higher than those of the inhibited solution throughout the immersion time, indicating the existence of a protective film on the corrosive surface. It is observed in Table 4 and Fig. 1 that IE declines with a growing time period from 12 to 72 hours. The phenomenon points out that the aggressive action of the acid medium was increasingly felt than the absorbance of the inhibitor, so desorption of the TTFE molecules (protective film) from MS surface occurs with the rise in the time period, this increased the area that will be available for corrosive attack, or we can say the corrosive solution of sulphuric acid can penetrate the inhibitor film and attack the steel surface [33,34].

Table 4. Gravimetric parameters for MS in 1.5N H_2SO_4 in various concentrations of TTFE at different times (h).

Conc. of inhib. w/v (%)	**12 hrs.**		**24 hrs.**		**48 hrs.**		**72 hrs.**	
	CR	IE%	CR	IE%	CR	IE%	CR	IE%
Blank	52.38	-	45.94	-	40.21	-	37.39	
0.12	14.04	73.19	16.47	64.15	16.19	59.72	15.87	57.56
0.24	10.06	80.80	10.48	77.18	12.67	68.49	12.92	65.44
0.36	7.74	85.22	7.37	83.95	9.66	75.98	10.24	72.62
0.48	6.76	87.09	5.86	87.24	6.78	83.14	6.71	82.05
0.60	5.72	89.08	4.85	89.44	5.55	86.20	5.60	85.01

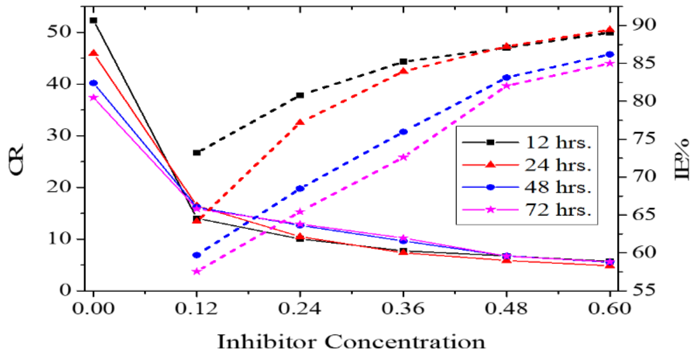

Figure 1. Effect of immersion time on corrosion of MS in 1.5N H_2SO_4 with TTFE at 30°C.

3.1.3. Effect of temperature.

The temperature effect on the gravimetric parameters for mild steel in 1.5N H_2SO_4 solution in the absence and the presence of TTFE at a temperature range 303K – 333K for 6 h immersion periods is displayed in Table 5. Corrosion rate and inhibition efficiency plots of MS with and without the addition of different concentrations of TTFE in 1.5N H_2SO_4 at 303-333K are shown in Fig.2. Table 5 shows that corrosion rate increased with increasing temperature both in uninhibited and inhibited solutions while the inhibition efficiencies decreased. This may be due to a decrease in the strength of the adsorption process at a higher temperature, suggesting the physisorption of the inhibitor sample on the MS surface [35-37].

Table 5. Gravimetric parameters for MS in 1.5N H_2SO_4 with various concentrations of TTFE at different temperatures.

Inhib. Conc.	CR				IE%			
w/v (%)	303K	313K	323K	333K	303K	313K	323K	333K
Blank	40.30	84.21	133.30	240.44	-	-	-	-
0.12	10.40	25.04	52.93	125.89	74.20	70.26	60.30	47.64
0.24	6.79	17.51	37.97	89.63	83.16	79.21	71.52	62.72
0.36	5.10	12.06	27.94	70.56	87.31	85.67	79.04	70.65
0.48	4.26	11.99	24.74	66.45	89.43	85.77	81.44	72.36
0.60	3.89	10.97	24.15	60.43	90.32	86.98	81.89	74.87

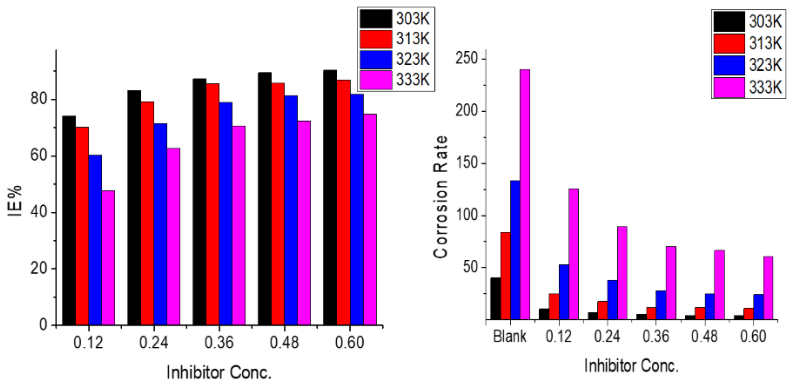

Figure 2. Effect of Temperature on corrosion of MS in 1.5N H_2SO_4 with TTFE at 6 hrs.

3.2. Adsorption isotherms.

Adsorption isotherms have a significant role in determining the mechanism of corrosion reactions.

Gravimetric results indicated that the increase in inhibition efficiency could be due to the inhibition effect occurring through the adsorption of the inhibitor molecule on the metallic surface. Inhibition efficiency is directly proportional to the adsorbed molecule's surface covered (θ).

3.2.1. Langmuir adsorption isotherm.

The Langmuir adsorption isotherm equation is:

$$\log\left(\frac{\theta}{1-\theta}\right) = \log C + \log K_{ads} \qquad \ldots(6)$$

Where C is inhibitor concentration, K_{ads} is adsorption equilibrium constant.

When plotting a logarithm graph of (θ/1-θ) against C, displayed a straight line as shown in Fig.3. The linear graph having a slope of about one and high correlation coefficients (R^2> 0.9) indicates that the adsorption process of TTFE on the mild steel surface follows the Langmuir adsorption isotherm [38]. The Langmuir isotherm indicates monolayer adsorption of the inhibitory molecule. The adsorption coefficient K_{ads} can be computed from the intercept of curves. This isotherm also indicates that organic components present in TTFE with polar atoms or groups adsorbed on the metallic surface can interact by mutual repulsion or attraction [39].

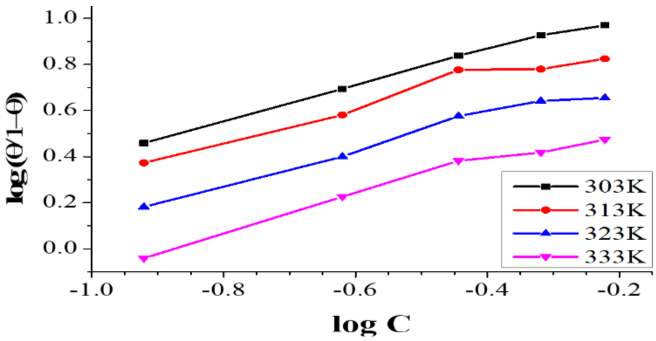

Figure 3. Langmuir adsorption isotherm curve for MS in 1.5N H_2SO_4 with TTFE (06h).

The free energy of adsorption (ΔG^0_{ads}) can be calculated using K_{ads} values with the help of the following equation [40]

$$\Delta G^0_{ads} = -RT\ln(55.5K_{ads}) \qquad \ldots (7)$$

Where, ΔG^0_{ads} is a change in Gibbs free energy, R is the universal gas constant (8.314 J K^{-1} mol^{-1}), T is absolute temp, and 55.5 is a concentration of water ($molL^{-1}$).

The negative values of ΔG^0_{ads} as shown in Table 6 favors the spontaneous process for the adsorption of inhibitor molecules on mild steel surfaces [41]. The negative values of ΔG^0_{ads} around 20 kJ/mol or less consistent with electrostatic interaction (physisorption) between the molecule of adsorbent and adsorbate [42].

Table 6. Adsorption Equilibrium constant and Gibbs free energy in 1.5N H_2SO_4 with TTFE at different temperatures.

Temperature (K)	R^2	K_{ads}	ΔG^0_{ads} (kJ/mol)
303	0.9941	0.9785	-10.06
313	0.9422	0.9535	-10.33
323	0.9692	0.9372	-10.61
333	0.9699	0.9005	-10.83

3.3. Thermodynamic parameters.

Thermodynamic parameters such as Activation energy (Ea), Enthalpy of Adsorption (ΔH^0_{ads}) and Entropy of Adsorption (ΔS^0_{ads}) were undertaken to know the mode of adsorption mechanism involved in the corrosion inhibition process. These parameters for corrosion of mild steel in 1.5N H_2SO_4 solutions in the absence and the presence of TTFE at 303–333 K were calculated from the Arrhenius equation (8) [43] and the transition state theory equation (9).

$$\ln(CR) = \ln A - \frac{E_a}{RT} \qquad ...(8)$$

Where CR = rate of corrosion,
A = the exponential factor,
E_a = activation energy,
R = Universal gas constant (8.314 J/Kmol) and
T = absolute temperature.

A plot of log CR vs. 1/T gave a straight line with the slope of (-Ea/2.303R). It intercepted (logA), as revealed in Fig.4. The values of activation energy in solutions containing TTFE were found to be higher than uninhibited solution as shown in Table-7. The increase in E_a in the presence of an inhibitor could be interpreted as physical adsorption [44].

$$\ln\frac{CR}{T} = \left(\ln\left\{\frac{R}{Nh}\right\} + \frac{\Delta S^0_{ads}}{R}\right) - \frac{\Delta H^0_{ads}}{RT} \qquad ... (9)$$

Where, h = Planck's constant (6.626176×10^{-34}Js),
N = Avogadro's number, (6.022×10^{23} mol^{-1}),

A plot of log CR/T against 1/T gave a straight line with a slope ($-\Delta H^0_{ads}/2.303R$) and an intercept (log R/Nh $+\Delta S^0_{ads}/2.303R$) are shown in Fig.5. The values of ΔH^0_{ads} and ΔS^0_{ads} were obtained from the slopes and intercept of the graph, respectively, and listed in Table 7.

The positive values of ΔH^0_{ads}revealed the endothermic nature of the adsorption of TTFE inhibitor on the MS dissolution process, and it can be suggested that the dissolution reaction was slow in the presence of the inhibitor [45]. The negative values of ΔS^0_{ads} in the absence and presence of an inhibitor, the activated Complex in the rate-determining step represents an association rather than a dissociation step, meaning that a decrease in disordering occurs from the reactant to the activated complex [46].

Table 7. Thermodynamic parameters for MS corrosion in 1.5N H_2SO_4 with TTFE.

Concentration of inhibitor w/v (%)	Activation Energy E_a (kJ/mol)	Enthalpy ΔH^0_{ads} (kJ/mol)	Entropy ΔS^0_{ads} (kJ/mol/K)
Blank	48.90	46.23	-0.219
0.12	69.06	66.42	-0.164
0.24	71.52	68.88	-0.159
0.36	73.13	70.49	-0.156
0.48	75.27	72.61	-0.150
0.60	75.77	73.11	-0.150

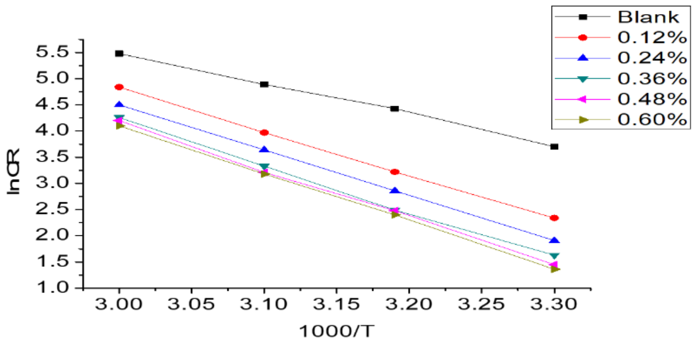

Figure 4. Arrhenius plots for MS corrosion in 1.5N H_2SO_4 with TTFE.

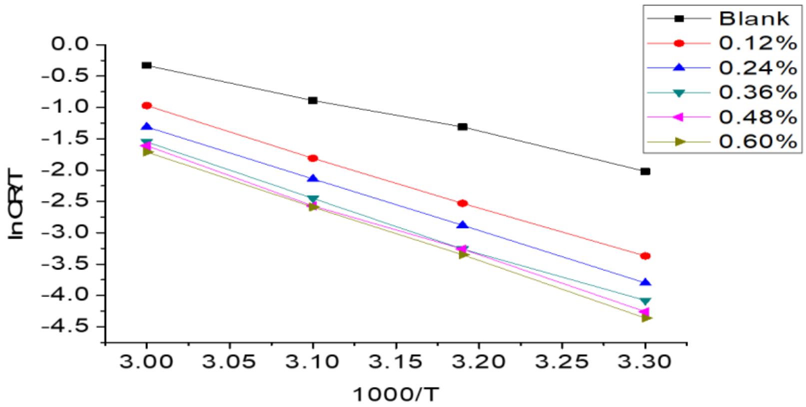

Figure 5. Transition state plots for MS corrosion in 1.5N H_2SO_4 with TTFE.

3.4. Kinetics of the corrosion process: Rate constant and half – life.

Kinetic data analysis is considered necessary since the corrosion reaction is a heterogeneous process composed of anodic and cathodic reactions at the same or different rates [47]. The kinetic analysis of the data supports the pseudo-first-order kinetics was employed and evaluated using an integral method of analysis by eq. 10 below [48]:

$$\mathrm{M}_t = M_i e^{-k_1 t} \quad \text{... (10)}$$

This equation can be written as-

$$\log(\mathrm{M}_t) = -\frac{k_1 t}{2.303} + \log(M_i) \quad \text{... (11)}$$

M_t = weight of coupons at time t after immersion

M_i = initial weight of coupons before immersion

k_1 = the pseudo-first-order rate constant (hr $^{-1}$)

t = Immersion time in hr

when $\log(\mathrm{M}_t)$ was plotted against time in hours, a linear variation was observed, as shown in Fig. 6, which confirms a pseudo-first-order reaction kinetics concerning the corrosion of mild steel in 1.5N H_2SO_4 solution in the presence and the absence of an inhibitor. The values of the rate constants obtained from the slopes of the plot in Fig. 5 are presented in Table 8.

The results reveal that the rate constant (k_1) decreases with an increase in the concentration of inhibitor and is highest for the uninhibited acid solution. This confirms the inhibition of mild steel corrosion in acid solution by inhibitors.

The half-life values, $t_{1/2}$, of the metal in the test solutions were calculated from the eq. 13 when $M_t = M_i/2$ at time $t = t_{1/2}$:

$$\frac{\mathrm{M}_t}{\mathrm{M}_i} = e^{-k_1 t} \quad \text{... (12)}$$

$$t_{1/2} = \frac{0.693}{k_1} \quad \text{...(13)}$$

and these data are also listed in Table 8. The half-life values are observed to increase with an increase in inhibitor concentration, indicating a decrease in the dissolution rate of the metal in the acid solution with increasing inhibitor concentration. It is, therefore, informative to assert that the presence of inhibitor extract increases the service life of the alloy [49].

The high value of the correlation coefficient obtained showed that the experimental value fitted well with the first-order kinetics [50].

Table 8. Kinetic parameters for MS corrosion in 1.5N H_2SO_4 with TTFE.

Inhibitor Conc. w/v (%)	Rate Constant (k) (x 10^{-3} hr^{-1})	Half-Life ($t_{1/2}$) (hr)	Correlation Coefficient (R^2)
Blank	22.68	30.55	0.9732
0.12	5.96	116.18	0.9972
0.24	4.65	148.97	0.9901
0.36	3.55	195.40	0.9848
0.48	2.22	311.67	0.9960
0.60	1.82	381.17	0.9960

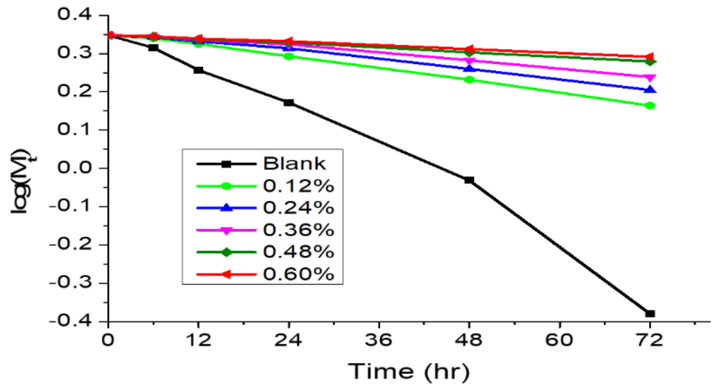

Figure 6. Plot of log(M_t) against time for MS coupons in 1.5N H_2SO_4 solution containing the TTFE.

3.5. Electrochemical measurement.

3.5.1. Potentiodynamic polarization measurements.

The inhibitor's anticorrosion behavior was analyzed through anodic and cathodic polarization by plotting a curve between corrosion current density and corrosion potential, known as the Tafel plot, which are shown in Fig.7. The experimental data's for Potentiodynamic parameters such as corrosion current density (I_{corr}), corrosion potential (E_{corr}), Tafel slopes ($ß_a$ and $ß_c$) and inhibition efficiency IE (%) for corrosion of MS in 1.5N H_2SO_4 containing different concentrations of TTFE at 303K are listed in Table 9. It is observed from the experimental values that the corrosion current density for the inhibited solution is smaller than that for the blank solution, which favors slowing down the corrosion process. The current density decreases when an inhibitor is added to the solution. This indicates that a protective layer is formed on the metal, reducing corrosion [51].

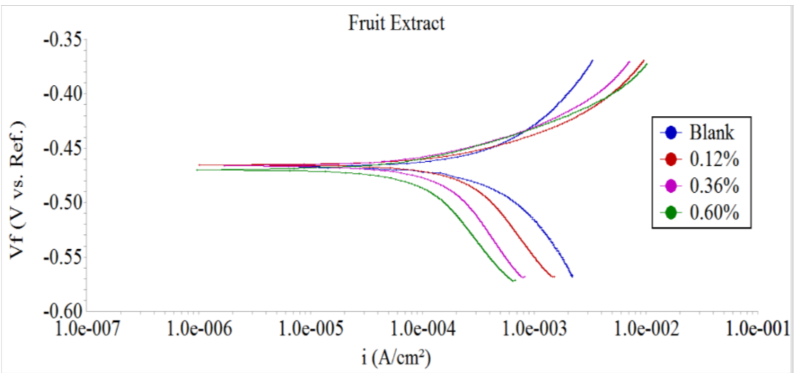

Figure 7. Tafel plots with and without TTFE in 1.5N H_2SO_4.

The shift in E_{corr} value has no definite trend in the presence of various concentrations of inhibitors, supporting the mixed type nature of inhibitor and simple geometric blocking mechanism of inhibition [52]. It influences both metal dissolution and hydrogen evolution.

The values of both Tafel slopes ($ß_a$ and $ß_c$) were also found to vary with TTFE concentration. This clarifies that the studied compound behaved as a mixed-type inhibitor [53].

Table 9. Potentiodynamic polarization parameters of MS in 1.5N H_2SO_4 at 303±1 K.

Conc. of inhibit w/v (%)	$-E_{corr}$ (mV)	i_{corr} ($\mu A/cm^2$)	β_a (mV/dec)	$-\beta_c$ (mV/dec)	CR (mmpy)	θ	IE (%)
Blank	467	919	158.0	243.2	10.716	-	-
0.12	465	330	53.6	181.1	3.848	0.6409	64.09
0.36	466	185	49.6	178.1	2.157	0.7987	79.87
0.60	470	131	46.5	169.6	1.528	0.8575	85.75

3.5.2. Electrochemical impedance spectroscopy.

The impedance behavior of MS in 1.5N H_2SO_4 solution containing different concentrations of TTFE is presented by complex impedance plots (Nyquist and Bode plot), as shown in Fig.8 and Fig. 9, respectively. The impedance parameters obtained using the Randle circuit via the EIS are presented in Table 10. This circuit is constituted of series solution resistance (R_s) with the parallel combination of charge transfer resistance R_{ct} and double layer capacitance $C_{dl.}$ The similar semi-circle shape of Nyquist curves is almost maintained in the predefined concentration range of the inhibitor, which suggests that no change in the mechanism of the corrosion process occurs when the plant extract is added [54]. The diameter of Nyquist plots increased with the increase in the concentration of inhibitor, which indicates an increase in impedance and the strengthening of inhibitor film on the metal surface [55].

Higher charge transfer resistance (R_{ct}) could be attributed to higher inhibitor efficiency [56]. The value of R_{ct} increases, whereas C_{dl} values decrease with the addition of inhibitor due to the increase in the thickness of the double layer and decrease in the dielectric constant. Consequently, it causes the rate of corrosion to decrease [57].

Table 10. Impedance parameters for MS in 1.5N H_2SO_4 at 303±1 K.

Concentration of inhibitor w/v (%)	R_{sol} ($\Omega.cm^2$)	R_{ct} ($\Omega.cm^2$)	C_{dl} ($\mu F\ cm^{-2}$)	θ	IE (%)
Blank	1.98	12.31	100.40	-	-
0.12	5.67	37.03	29.04	0.6676	66.76
0.36	7.47	54.03	40.56	0.7722	77.22
0.60	8.87	90.41	17.66	0.8638	86.38

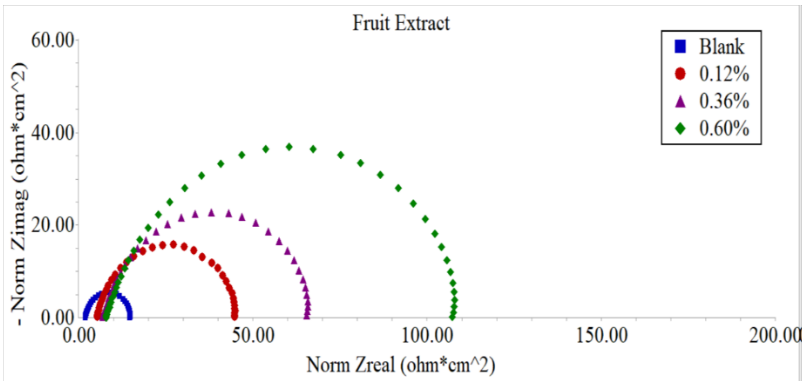

Figure 8. Nyquist curve for MS in absence and presence of different concentrations of TTFE in 1.5N H_2SO_4.

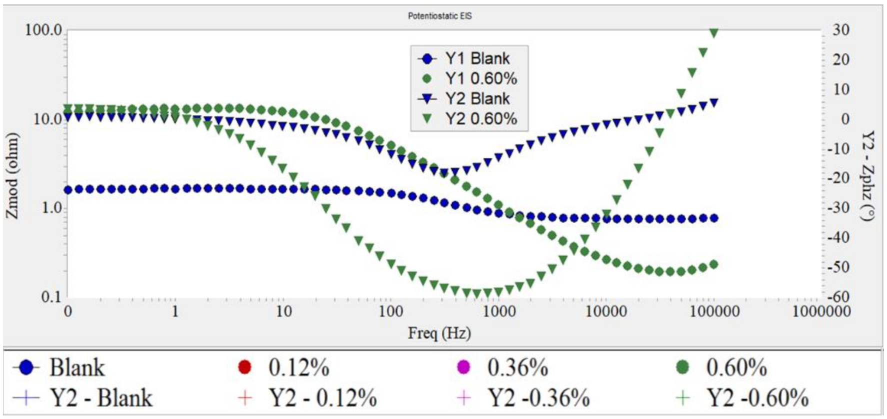

Figure 9. Bode curve for MS in the absence and presence of different concentrations of TTFE in 1.5N H_2SO_4.

3.6. SEM analysis.

The surface morphology of MS coupons was studied through Scanning Electron Microscope (SEM) images of magnification (x10000). The SEM images (Fig.10a) show the plain untreated mild steel, (Fig.10b) MS after immersion in 1.5N H_2SO_4 for 24 hours, while (Fig.10c) reveals 0.60% fruit extract of *Tribulus terrestris*, respectively. The smooth metal surface (Fig.10a) of untreated metal indicates the absence of any corrosion product on it.

Comparing Fig.10b with Fig.10c at the same magnifications, it can be seen that it has more roughness with pits and cracks in Fig.10b because of being badly attacked by a corrosive environment, has almost disappeared in Fig.10c, and MS surface is almost free from corrosion in acidic solution due to the MS surface covered by the TTFE inhibitor.

TTFE can decrease the corrosion rate in an acidic environment because the protective layer it forms covers more surface area of the metal surface, which is responsible for the corrosion inhibition process. These observations are in agreement with the findings [58].

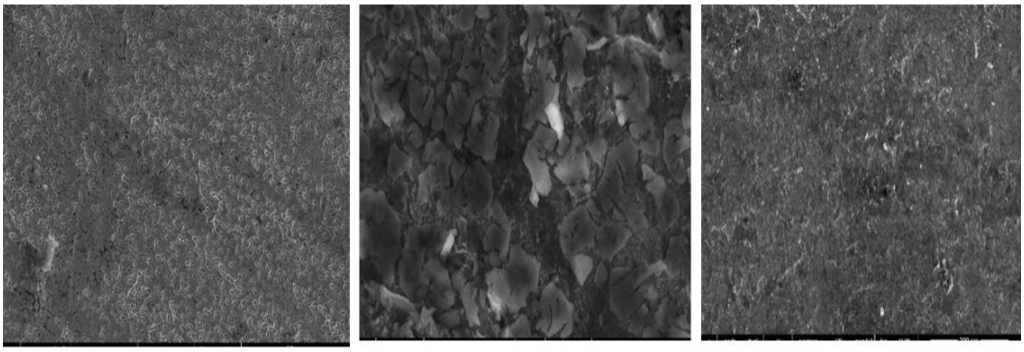

(a) (b) (c)

Figure 10. SEM images of MS (a) polished MS (b) MS in H_2SO_4 (blank) (c) MS in 1.5N H_2SO_4 with 0.60%.

4. Conclusions

In this study, the plant extract *TTFE* was shown to be an effective mixed-type corrosion inhibitor for mild steel (MS) in a sulphuric acid medium. The inhibition efficiency increased with the concentration of the inhibitor but decreased with rising temperatures from 303K to 333K, with the maximum efficiency observed at 0.60% inhibitor concentration at 303K. The corrosion rate in the blank solution was consistently higher than in the inhibited solution for all immersion times, indicating that a protective film formed on the MS surface, reducing corrosion over time.

The adsorption of *TTFE* followed the Langmuir isotherm, suggesting a monolayer adsorption mechanism. Thermodynamic analysis showed that the corrosion reactions were endothermic, supported by positive enthalpy values, while negative entropy suggested an associative mechanism. The negative Gibbs free energy confirmed the spontaneous nature of the adsorption process.

Kinetic studies showed that the inhibition process followed a pseudo-first-order reaction characterized by physical adsorption, the increasing half-life times with higher concentrations indicated a slower metal dissolution in the acid solution, further supporting the inhibitor's efficacy. Impedance spectroscopy revealed an increase in corrosion resistance due to the protective layer formed by the extract. Tafel analysis also confirmed the mixed-type inhibition behavior of *TTFE*, affecting both the anodic and cathodic reactions.

Surface morphology studies, particularly SEM, provided visual confirmation of the protective film formed on the MS surface, complementing the electrochemical data. The results from various methods, including impedance and polarization studies, were consistent and mutually supportive, reinforcing the conclusion that *TTFE* is an effective corrosion inhibitor for mild steel in sulphuric acid environments.

Funding

This research received no external funding.

Acknowledgments

This research has no acknowledgment.

Conflicts of Interest

The authors declare no conflict of interest.

References

1. Oli, H.B.; Parajuli, D.L.; Sharma, S.; Chapagain, A.; Yadav, A.P. Adsorption Isotherm and Activation Energy of Inhibition of Alkaloids on Mild Steel Surface in Acidic Medium. *Amrit Research Journal* **2021**, *2*, 59-67, https://doi.org/10.3126/arj.v2i01.40738.
2. Dwivedi, D.; Lepková, K.; Becker, T. Carbon steel corrosion: a review of key surface properties and characterization methods. *RSC Advances* **2017**, *7*, 4580-4610, https://doi.org/10.1039/C6RA25094G.
3. Mostafatabar, A.H.; Bahlakeh, G.; Ramezanzadeh, B.; Dehghani, A.; Ramezanzadeh, M. A comprehensive electronic-scale DFT modeling, atomic-level MC/MD simulation, and electrochemical/surface exploration of active nature-inspired phytochemicals based on Heracleum persicum seeds phytoextract for effective retardation of the acidic-induced corrosion of mild steel. *Journal of Molecular Liquids* **2021**, *331*, https://doi.org/10.1016/j.molliq.2021.115764.
4. Wang, J.; Jing, J.; Feng, L.; Zhu, H.; Hu, Z.; Ma, X. Study on corrosion inhibition behavior and adsorption mechanism of novel synthetic surfactants for carbon steel in 1 M HCl solution. *Sustainable Chemistry and Pharmacy* **2021**, *23*, https://doi.org/10.1016/j.scp.2021.100500.
5. Sang, Y.; Liu, Q.; Wang, S.; Dong, S.; Fan, Y.; Zhao, X.; Li, S. Synthetic polyaniline-boron nitride-aqueous epoxy resin composite coating for improving the corrosion resistance of hot-dip galvanized steel plates. *Applied Surface Science* **2022**, *592*, https://doi.org/10.1016/j.apsusc.2022.153229.
6. Echihi, S.; Benzbiria, N.; Belghiti, M.E.; El Fal, M.; Boudalia, M.; Essassi, E.M.; Guenbour, A.; Bellaouchou, A.; Tabyaoui, M.; Azzi, M. Corrosion inhibition of copper by pyrazole pyrimidine derivative in synthetic seawater: Experimental and theoretical studies. *Materials Today: Proceedings* **2021**, *37*, 3958-3966, https://doi.org/10.1016/j.matpr.2020.09.264.
7. Abdelaziz, S.; Benamira, M.; Messaadia, L.; Boughoues, Y.; Lahmar, H.; Boudjerda, A. Green corrosion inhibition of mild steel in HCl medium using leaves extract of Arbutus unedo L. plant: An experimental and computational approach. *Colloids and Surfaces A: Physicochemical and Engineering Aspects* **2021**, *619*, https://doi.org/10.1016/j.colsurfa.2021.126496.

8. Wan, S.; Zhang, T.; Chen, H.; Liao, B.; Guo, X. Kapok leaves extract and synergistic iodide as novel effective corrosion inhibitors for Q235 carbon steel in H2SO4 medium. *Industrial Crops and Products* **2022**, *178*, https://doi.org/10.1016/j.indcrop.2022.114649.
9. Soltani, N.; Tavakkoli, N.; Khayatkashani, M.; Eslami, E. Curcuma Zedoaria Extract as a Novel Corrosion Inhibitor for Mild Steel in 0.5 M H2SO4. *Iranian Journal of Analytical Chemistry* **2022**, *9*, 27-39, https://doi.org/10.30473/IJAC.2022.63029.1226.
10. Chaudhary, S.; Tak, R.K. Tribulus terrestris Extracts: An Eco-Friendly Corrosion Inhibitor for Mild Steel in H 2 SO 4 Medium. *Asian J. Chem.* **2017**, *29*, https://doi.org/10.14233/ajchem.2017.20702.
11. Al Maofaria, A.; Doucha, S.; Benmessaouda, M.; Hajjaji, S.E.L.; Mosaddak, M.; Ouaki, B. Inhibition Study of Various Extracts of Tribulus Terrestris Plant on the Corrosion of Mild Steel in a 1.0 M HCl Solution. *Port. Electrochimica Acta* **2021**, *39*, 21-35.
12. Al-Moubaraki, A.H.; Al-Malwi, S.D. Experimental and theoretical evaluation of aqueous black mustard seeds extract as sustainable-green inhibitor for mild steel corrosion in H2SO4 acid solutions. *Journal of Adhesion Science and Technology* **2022**, 1-32, https://doi.org/10.1080/01694243.2022.2062955.
13. Rathod, M.R.; Minagalavar, R.L.; Rajappa, S.K. Effect of Artabotrys odoratissimus extract as an environmentally sustainable inhibitor for mild steel corrosion in 0.5 M H2SO4 media. *Journal of the Indian Chemical Society* **2022**, *99*, https://doi.org/10.1016/j.jics.2022.100445.
14. Sannaiah, P.N.; Alva, V.D.P.; Bangera, S. An experimental, theoretical, and spectral approach to evaluating the effect of eco-friendly Oxalis stricta leaf extract on the corrosion inhibition of mild steel in 1 N H2SO4 medium. *Journal of the Iranian Chemical Society* **2022**, *19*, 1817-1835, https://doi.org/10.1007/s13738-021-02422-6.
15. Abdulqawi, L.N.; Quadri, S.A.; Evaluation of Antibacterial and Antioxidant activities of Tribulus terrestris L. Fruits. *Research Journal of Pharmacy and Technology* **2021**, *14,* https://doi.org/10.5958/0974-360X.2021.00061.5.
16. Gibbons, S. Plants as a Source of Bacterial Resistance Modulators and Anti-Infective Agents. *Phytochemistry Reviews* **2005**, *4*, 63-78, https://doi.org/10.1007/s11101-005-2494-9.
17. Sørum, H.; L'Abée-Lund, T.M. Antibiotic resistance in food-related bacteria—a result of interfering with the global web of bacterial genetics. *International Journal of Food Microbiology* **2002**, *78*, 43-56, https://doi.org/10.1016/S0168-1605(02)00241-6.
18. White, D.G.; Zhao, S.; Simjee, S.; Wagner, D.D.; McDermott, P.F. Antimicrobial resistance of foodborne pathogens. *Microbes and Infection* **2002**, *4*, 405-412, https://doi.org/10.1016/S1286-4579(02)01554-X.
19. Duke, J.A.; Bogenschutz-Godwin, M.J.; Duke, P.A.K. *Duke Handbook of medicinal herbs*. 2nd edn. United States: CRC Press, **2002**; pp. 595, http://localhost:8080/xmlui/handle/123456789/73.
20. Vasait Rajendrabhai, D. Detection of phytochemical and pharmacological properties of crude extracts of Tribulus terrestris collected from tribal regions of Baglan (MS), India. *Int. J. Pharmacognosy Phytochem. Res.* **2017**, *9*, 508-511.
21. Abirami, P. and Rajendran, A.; GC-MS Analysis of Tribulus terrestris. *Asian J. Plant Sci. Res.* **2011**, *1*, 13-16.
22. Tyagi, P.; Ranjan, R. Comparative study of the pharmacological, phytochemical and biotechnological aspects of Tribulus terrestris Linn. and Pedalium murex Linn: An overview. *Acta Ecologica Sinica* **2021**, https://doi.org/10.1016/j.chnaes.2021.07.008.
23. Rashed, S.A.; Eldarier, S.M.; El-Sheikh, A.A.; Toto, S.M. Ethno-phytotechnology of Tribulus terrestris L. (Zygophyllaceae). *Egyptian Journal of Botany* **2022**, *62*, 561-573, https://doi.org/10.21608/ejbo.2022.114629.1874.
24. Barmatov, E.; Geddes, J.; Hughes, T. and Nagl, M.; March. Research on corrosion inhibitors for acid stimulation. Paper presented at the *Corros.* In: NACE, C2012 – 0001573. 2012, Salt Lake City, Utah, March **2012**.
25. Chaudhary, S.; Kumari, K. Influence of gokhru leaves extract on corrosion inhibition of aluminium in acidic medium. *J. Adv. Sci. Res.*, **2021,** *12*, 288-291.
26. Sivaraju, M.; Kannan, K. Eco-friendly Inhibitor (Tribulus terrestris L) for Mild Steel Corrosion in 1 N Phosphoric Acid. *Asian Journal of Chemistry* **2010**, *22*, 233-244.
27. Chaudhary, S.; Tak, R.K. Natural corrosion inhibition and adsorption characteristics of tribulus terrestris plant extract on aluminium in hydrochloric acid environment. *Biointerface Res. Appl. Chem*. **2022**, *12*, 2603-2617, https://doi.org/10.33263/BRIAC122.26032617.
28. Aralu, C.C.; Chukwuemeka-Okorie, H.O.; Akpomie, K.G. Inhibition and adsorption potentials of mild steel corrosion using methanol extract of Gongronema latifoliuim. *Applied Water Science* **2021**, *11*, 1-7, https://doi.org/10.1007/s13201-020-01351-8.
29. Jones, D.A. *Principles and Prevention of Corrosion*. 2nd edn Prentice-Hall **1996**.
30. Zhang, Q.; Hua, Y. Corrosion inhibition of aluminum in hydrochloric acid solution by alkylimidazolium ionic liquids. *Materials Chemistry and Physics* **2010**, *119*, 57-64, https://doi.org/10.1016/j.matchemphys.2009.07.035.

31. Ben Aoun, S. On the corrosion inhibition of carbon steel in 1 M HCl with a pyridinium-ionic liquid: chemical, thermodynamic, kinetic and electrochemical studies. *RSC Advances* **2017**, *7*, 36688-36696, https://doi.org/10.1039/C7RA04084A.
32. Rabizadeh, T.; Asl, S.K. Casein as a natural protein to inhibit the corrosion of mild steel in HCl solution. *Journal of Molecular Liquids* **2019**, *276*, 694-704, https://doi.org/10.1016/j.molliq.2018.11.162.
33. Shaker, L.M.; Al-Adili, A.; Al-Amiery, A.A.; Takriff, M.S. The inhibition of mild steel corrosion in 0.5 M H2SO4 solution by N-phenethylhydrazinecarbothioamide (N-PHC). *J. Phys. Conf. Ser.* **2021,** *1795*, https://doi.org/10.1088/1742-6596/1795/1/012009.
34. Akinbulumo, O.A.; Odejobi, O.J.; Odekanle, E.L. Thermodynamics and adsorption study of the corrosion inhibition of mild steel by Euphorbia heterophylla L. extract in 1.5 M HCl. *Results in Materials* **2020**, *5*, https://doi.org/10.1016/j.rinma.2020.100074.
35. Ebenso, E.E.; Obot, I.B.; Murulana, L.C. Quinoline and its derivatives as effective corrosion inhibitors for mild steel in acidic medium. *Int. J. Electrochem. Sci*. **2010**, *5*, 1574-1586.
36. Saraswat, V.; Kumari, R.; Yadav, M. Novel carbon dots as efficient green corrosion inhibitor for mild steel in HCl solution: Electrochemical, gravimetric and XPS studies. *Journal of Physics and Chemistry of Solids* **2022**, *160*, https://doi.org/10.1016/j.jpcs.2021.110341.
37. Resen, A.; Hanoon, M.; Alani, W.K.; Kadhum, A.; Mohammed, A.; Gaaz, T.; Kadhum, A.; Al-Amiery, A.; Takriff, M.; Resen, A. Exploration of 8-piperazine-1-ylmethylumbelliferone for application as a corrosion inhibitor for mild steel in hydrochloric acid solution. *International Journal of Corrosion and Scale Inhibition* **2021**, *10*, 368–387, https://doi.org/10.17675/2305-6894-2021-10-1-21.
38. Chaudhary, S.; Tak, R.; Duchaniya, R.K. Corrosion Inhibition of Mild Steel in 0.5N H2SO4 Solution by Tribulus terrestris (fruit) Extract. *Journal of Surface Science and Technology* **2017**, *33*, 63-69, https://doi.org/10.18311/jsst/2017/15575.
39. Pradeep Kumar C B, D. Adsorption and Thermodynamic Characteristics of Plumeria rubra Plant Extracts on Mild Steel Corrosion in Industrial Water Medium. *International Research Journal of Pure and Applied Chemistry* **2014**, *3*, 330-346.
40. Ayoola, A.A.; Babalola, R.; Durodola, B.M.; Alagbe, E.E.; Agboola, O.; Adegbile, E.O. Corrosion inhibition of A36 mild steel in 0.5 M acid medium using waste citrus limonum peels. *Results in Engineering* **2022**, *15*, https://doi.org/10.1016/j.rineng.2022.100490.
41. Kadhim, A.; Betti, N.; Al-Bahrani, H.A.; Al-Ghezi, M.K.S.; Gaaz, T.; Kadhum, A.H.; Alamiery, A. A mini review on corrosion, inhibitors and mechanism types of mild steel inhibition in an acidic environment. *Int. J. Corros. Scale Inhib.* **2021**, *10*, 861-884, https://doi.org/10.17675/2305-6894-2021-10-3-2.
42. Aysel, B.; Meltem, D. The Use of papaver somniferum L. Plant Extract as Corrosion Inhibitor. *Protection of Metals and Physical Chemistry of Surfaces* **2019**, *55*, 1182-1194, https://doi.org/10.1134/S2070205119060042.
43. Xia, S.; Luo, Y.; Li, Y.; Liu, W.; Ding, X.; Tang, L. Effects of Temperature on Corrosion Behavior of Reinforcements in Simulated Sea-Sand Concrete Pore Solution. *Buildings* **2022**, *12*, https://doi.org/10.3390/buildings12040407.
44. Obot, I.; Ebenso, E.; Gasem, Z. Eco-friendly Corrosion Inhibitors: Adsorption and Inhibitive Action of Ethanol Extracts of Chlomolaena Odorata L. for the Corrosion of Mild Steel in H 2 SO 4 Solutions. *International Journal of Electrochemical Science* **2012**, *7*, 1997-2008.
45. Mu, G.N.; Li, X.; Li, F. Synergistic inhibition between o-phenanthroline and chloride ion on cold rolled steel corrosion in phosphoric acid. *Materials Chemistry and Physics* **2004**, *86*, 59-68, https://doi.org/10.1016/j.matchemphys.2004.01.041.
46. Behpour, M.; Ghoreishi, S.M.; Khayatkashani, M.; Soltani, N. The effect of two oleo-gum resin exudate from Ferula assa-foetida and Dorema ammoniacum on mild steel corrosion in acidic media. *Corrosion Science* **2011**, *53*, 2489-2501, https://doi.org/10.1016/j.corsci.2011.04.005.
47. Olasehinde, E.; J. Olusegun, S.; Adesina, A.; Omogbehin, S.A.; Chahul, H. Inhibitory Action of Nicotiana tabacum Extracts on the Corrosion of Mild Steel in HCl: Adsorption and Thermodynamics Study. *Nature and Science* **2012**, *11*, 83-90.
48. Okewale, A.O.; Adesina, O.A. Kinetics and thermodynamic study of corrosion inhibition of mild steel in 1.5 M HCl medium using cocoa leaf extract as inhibitor. *J. Appl. SCI. Environ. Manag.* **2020**, *24*, 37-47, https://dx.doi.org/10.4314/jasem.v24i1.6.
49. Ofuyekpone, O.D.; Utu, O.G.; Onyekpe, B.O. Corrosion inhibition for alloy 304L (UNS S30403) in H2SO4 1M solution by Centrosema pubescens leaves extract. *Applied Surface Science Advances* **2021**, *3*, https://doi.org/10.1016/j.apsadv.2021.100061.
50. Ijuo, G.A.; Chahul, H.F.; Eneji, I.S. Corrosion inhibition and adsorption behavior of Lonchocarpus laxiflorus extract on mild steel in hydrochloric acid, Ew. *J. Chem. Kine* **2016**, *1*, 21-30.
51. Iroha, N.B.; Nnanna, L.A. Electrochemical and Adsorption Study of the anticorrosion behavior of Cefepime on Pipeline steel surface in acidic Solution. *J. Mater. Environ. Sci.* **2019**, *10*, 898-908.
52. Raviprabha, K.; Ramesh, S.B. 5-(3-Pryridyl)-4H-1,2,4-triazole-3-thiol as Potential Corrosion Inhibitor for AA6061 Aluminium Alloy in 0.1 M Hydrochloric Acid Solution. *Surface Engineering and Applied Electrochemistry* **2019**, *55*, 723-733, https://doi.org/10.3103/S1068375519060103.

53. Nnanna, L.A.; Owate, I.O.; Oguzie, E.E.; Inhibition of mild steel corrosion in HCl solution by pentaclethra macrophylla bentham extract. *Int. J. Mater. Eng.* **2014,** *4*, 171-179.
54. Labjar, N.; Lebrini, M.; Bentiss, F.; Chihib, N.-E.; Hajjaji, S.E.; Jama, C. Corrosion inhibition of carbon steel and antibacterial properties of aminotris-(methylenephosphonic) acid. *Materials Chemistry and Physics* **2010**, *119*, 330-336, https://doi.org/10.1016/j.matchemphys.2009.09.006.
55. Gomes, M.P.; Costa, I.; Pébère, N.; Rossi, J.L.; Tribollet, B.; Vivier, V. On the corrosion mechanism of Mg investigated by electrochemical impedance spectroscopy. *Electrochimica Acta* **2019**, *306*, 61-70, https://doi.org/10.1016/j.electacta.2019.03.080.
56. Noreen, H.; Semmar, N.; Farman, M.; McCullagh, J.S.O. Measurement of total phenolic content and antioxidant activity of aerial parts of medicinal plant Coronopus didymus. *Asian Pacific Journal of Tropical Medicine* **2017**, *10*, 792-801, https://doi.org/10.1016/j.apjtm.2017.07.024.
57. Kumar, R.; Chahal, S.; Dahiya, S.; Dahiya, N.; Kumar, S.; Lata, S. Experimental and theoretical approach to exploit the corrosion inhibition activity of 3-formyl chromone derivatives on mild steel in 1 m H2SO4. *Corros. Rev.* **2017**, *35*, 95-110, https://doi.org/10.1515/corrrev-2017-0029.
58. Okewale, A.O.; Onocha, O.O.; Evawere, U.J. Corrosion Inhibition Of Carbon Steel In Saline And Carbon Dioxide Saturated Saline Solutions Using Pumpkin Pod Extract As Inhibitor. *FUW Trends Sci. Technol. J.* **2021**, *6*, 203–212.